Chinese Journal of Physiology 58(3): 178-187, 2015
DOI: 10.4077/CJP.2015.BAD298

Effect of Antidepressant Doxepin on Ca^{2+} Homeostasis and Viability in PC3 Human Prostate Cancer Cells

Ti Lu[1, #], Chiang-Ting Chou[2, 3, #], Wei-Zhe Liang[4], Chia-Cheng Yu[5], Hong-Tai Chang[5], Chun-Chi Kuo[6], Wei-Chuan Chen[7], Daih-Huang Kuo[8], Chin-Man Ho[4], Pochuen Shieh[8], and Chung-Ren Jan[4]

[1]*Department of Psychiatry, Kaohsiung Veterans General Hospital, Kaohsiung 81362*
[2]*Department of Nursing, Division of Basic Medical Sciences, Chang Gung Institute of Technology Chia-Yi 61363*
[3]*Chronic Diseases and Health Promotion Research Center, Chang Gung Institute of Technology Chia-Yi 61363*
[4]*Department of Medical Education and Research, Kaohsiung Veterans General Hospital Kaohsiung 81362*
[5]*Department of Surgery, Kaohsiung Veterans General Hospital, Kaohsiung 81362*
[6]*Department of Nursing, Tzu Hui Institute of Technology, Pingtung 92641*
[7]*Division of Surgery, St. Joseph Hospital, Kaohsiung 80288*
and
[8]*Department of Pharmacy, Tajen University, Pingtung 90741, Taiwan, Republic of China*

Abstract

The effect of the antidepressant doxepin on cytosolic Ca^{2+} concentrations ($[Ca^{2+}]_i$) and viability in PC3 human prostate cancer cells was explored. The Ca^{2+}-sensitive fluorescent dye fura-2 was applied to measure $[Ca^{2+}]_i$. Doxepin at concentrations of 500-1000 μM induced a $[Ca^{2+}]_i$ rise in a concentration-dependent manner. The response was reduced partly by removing Ca^{2+}. Doxepin-evoked Ca^{2+} entry was suppressed by Ca^{2+} entry blockers (nifedipine, econazole, SK&F96365), and protein kinase C (PKC) modulators. In the absence of extracellular Ca^{2+}, incubation with the endoplasmic reticulum Ca^{2+} pump inhibitor thapsigargin or 2,5-di-tert-butylhydroquinone (BHQ) partly inhibit doxepin-induced $[Ca^{2+}]_i$ rise. Incubation with doxepin nearly inhibited thapsigargin or BHQ-induced $[Ca^{2+}]_i$ rise. Inhibition of phospholipase C (PLC) with U73122 failed to alter doxepin-induced $[Ca^{2+}]_i$ rise. At concentrations of 200-250 μM, doxepin killed cells in a concentration-dependent manner. This cytotoxic effect was not reversed by chelating cytosolic Ca^{2+} with 1,2-bis(2-aminophenoxy)ethane-N,N,N',N'-tetraacetic acid/acetoxy methyl (BAPTA/AM). Annexin V/PI staining data implied that doxepin (200 and 250 μM) did not induce apoptosis. Collectively, in PC3 cells, doxepin induced a $[Ca^{2+}]_i$ rise by evoking PLC-independent Ca^{2+} release from stores including the endoplasmic reticulum and Ca^{2+} entry *via* PKC-sensitive store-operated Ca^{2+} channels. Doxepin caused cell death that was independent of $[Ca^{2+}]_i$ rises.

Key Words: Ca^{2+}, doxepin, endoplasmic reticulum, human prostate cancer cells, phospholipase C, protein kinase C

Corresponding authors: [1] Dr. Pochuen Shieh, Department of Pharmacy, Tajen University, Pingtung 90741, Taiwan; and [2] Dr. Chung-Ren Jan, Department of Medical Education and Research, Kaohsiung Veterans General Hospital, Kaohsiung 81362, Taiwan, R.O.C. Tel: +886-7-3422121 ext. 1509, Fax: +886-7-3468056, E-mail: crjan@isca.vghks.gov.tw
[#]Contributed equally to this work.
Received: May 26, 2014; Revised: July 15, 2014; Accepted: August 8, 2014.
 ISSN : 0304-4920. http://www.cps.org.tw

Introduction

Doxepin is a tricyclic antidepressant which might affect both serotonin and norepinephrine neurotransmission (36). The indications of doxepin are major depressive disorder, nocturnal enuresis, panic disorder, irritable bowel syndrome, migraine, chronic pain, neuralgia, and symptoms of attention-deficit/hyperactivity disorder (14). The effects of doxepin on histaminergic and 5-HT_{2A} receptors may be responsible for its sleep-improving effect (31). The most common side effects include dry mouth, sedation, constipation, increased appetite, and a rapid or irregular heartbeat.

The *in vitro* effect of doxepin is largely unclear. It has been shown that doxepin caused toxicity in dorsal root ganglion cells (16) and inhibited respiration of malignant glioma cells (18). Additionally, doxepin was shown to inhibit the HERG potassium channel (12), neuronal sodium channels (25), three subtypes of GABA transporter (24), cyclic AMP production (17), and monoamine oxidase (28). Regarding Ca^{2+} signaling, it has been shown that H1 histamine receptor antagonist doxepin inhibited the histamine-induced $[Ca^{2+}]_i$ rise in Jurkat cells and cloned human T lymphocytes (23).

Ca^{2+} ions play a crucial role in different biological responses. A rise in intracellular free Ca^{2+} concentrations ($[Ca^{2+}]_i$) can initiate many pathophysiological cellular processes (1). However, a unregulated $[Ca^{2+}]_i$ rise may cause ion flux, dysfunction of proteins, apoptosis, and proliferation, *etc.* (9). In order to explore the effect of doxepin on $[Ca^{2+}]_i$ in cells, the PC3 human prostate cancer cells were chosen. The PC3 cell line is commonly applied for prostate cancer research. It has been shown that in this cell, $[Ca^{2+}]_i$ can increase in response to the stimulation of various ligands such as MK-886 (19), desipramine (5), and safrole (4). Because doxepin may have pathophysiological effect in different cell types, our study was aimed to explore the effect of doxepin on PC3 cells.

Fura-2 was used as a fluorescent Ca^{2+}-sensitive dye to measure $[Ca^{2+}]_i$ changes in the present study. It was shown that doxepin induced both Ca^{2+} entry and Ca^{2+} release in PC3 cells. The $[Ca^{2+}]_i$ rises were characterized, the concentration-response plots were established, and the pathways underlying doxepin-evoked Ca^{2+} entry and Ca^{2+} release were explored. The effect of doxepin on cell viability was investigated by using the tetrazolium assay. The involvement of apoptosis was explored by using Annexin V/propidium iodide staining.

Materials and Methods

Materials

The reagents for cell culture were from Gibco® (Gaithersburg, MD, USA). Fura-2/AM and 1,2-bis(2-aminophenoxy)ethane-N,N,N',N'-tetraacetic acid/acetoxy methyl (BAPTA/AM) were from Molecular Probes® (Eugene, OR, USA). Doxepin and all other reagents were from Sigma-Aldrich® (St. Louis, MO, USA) unless otherwise indicated. The concentrations chosen for nifedipine, econazole, SK&F96365, PMA, GF109203X, thapsigargin, BHQ, U73122, and ATP were based on literature and were effective in interacting with the targets of these chemicals.

Cell Culture

PC3 human prostate cancer cells, MG63 human osteosarcoma cells and DBTRG-05MG human glioblastoma cells obtained from Bioresource Collection and Research Center (Taiwan) were cultured in RPMI-1640 medium or Minimum Essential Medium (MEM) supplemented with 10% heat-inactivated fetal bovine serum, 100 U/ml penicillin and 100 μg/ml streptomycin.

Solutions Used in $[Ca^{2+}]_i$ Measurements

Ca^{2+}-containing medium (pH 7.4) had 140 mM NaCl, 5 mM KCl, 1 mM $MgCl_2$, 2 mM $CaCl_2$, 10 mM HEPES, and 5 mM glucose. Ca^{2+}-free medium contained similar components as Ca^{2+}-containing medium except that $CaCl_2$ was omitted and 2 mM $MgCl_2$/0.3 mM *ethylene glycol tetraacetic acid* (EGTA) were added. Doxepin was dissolved in water as a 1 M stock solution. The other chemicals were dissolved in water, ethanol or dimethyl sulfoxide. The concentration of organic solvents in the solution used in experiments did not exceed 0.1%, and did not alter viability, basal $[Ca^{2+}]_i$, or apoptosis measurements.

$[Ca^{2+}]_i$ Measurements

Confluent cells grown on 6 cm dishes were trypsinized and made into a suspension in culture medium at a density of 10^6/ml. Cell viability was determined by trypan blue exclusion. The viability was usually greater than 95% after the treatment. Cells were subsequently loaded with 2 μM fura-2/AM for 30 min at 25°C in the same medium. After loading, cells were washed with Ca^{2+}-containing medium twice and was made into a suspension in Ca^{2+}-containing medium at a density of 10^7/ml. Fura-2 fluorescence measurements were performed in a water-jacketed cuvette (25°C) with continuous stirring; the cuvette contained 1 ml of medium and 0.5 million cells. Fluorescence was monitored with a Shimadzu RF-5301PC spectrofluorophotometer immediately

after 0.1 ml cell suspension was added to 0.9 ml Ca^{2+}-containing or Ca^{2+}-free medium, by recording excitation signals at 340 nm and 380 nm and emission signal at 510 nm at 1-sec intervals. During the recording, reagents were added to the cuvette by pausing the recording for 2 sec to open and close the cuvette-containing chamber. For calibration of $[Ca^{2+}]_i$, after completion of the experiments, the detergent Triton X-100 (0.1%) and $CaCl_2$ (5 mM) were added to the cuvette to obtain the maximal fura-2 fluorescence. Then the Ca^{2+} chelator *ethylene glycol tetraacetic acid* (10 mM) was added to chelate Ca^{2+} in the cuvette to obtain the minimal fura-2 fluorescence. $[Ca^{2+}]_i$ was calculated as previously described (6-8, 15). Cell viability remained >95% after 20 min of $[Ca^{2+}]_i$ measurements.

Cell Viability Assays

The measurement of cell viability was based on the ability of cells to cleave tetrazolium salts by dehydrogenases. Augmentation in the amount of developed color directly correlated with the number of live cells. Assays were performed according to manufacturer's instructions designed for this assay (Roche Molecular Biochemical, Indianapolis, IN, USA). Cells were seeded in 96-well plates at a density of 10,000 cells/well in culture medium for 24 h in the presence of doxepin. The cell viability detecting reagent 4-[3-[4-Iodophenyl]-2-4(4-nitrophenyl)-2H-5-tetrazolio-1,3-benzene disulfonate] (WST-1; 10 μl pure solution) was added to samples after doxepin treatment, and cells were incubated for 30 min in a humidified atmosphere. In experiments using BAPTA/AM to chelate cytosolic Ca^{2+}, cells were treated with 10 μM BAPTA/AM for 1 h prior to incubation with doxepin. The cells were washed once with Ca^{2+}-containing medium and incubated with/without doxepin for 24 h. The absorbance of samples (A_{450}) was determined using an enzyme-linked immunosorbent assay (ELISA) reader. Absolute optical density was normalized to the absorbance of unstimulated cells in each plate and expressed as a percentage of the control value.

Alexa ®Fluor 488 Annexin V/PI Staining for Detection of Apoptosis

Annexin V/PI staining assay (7, 37) was employed to further detect PC3 cells in early apoptosis/necrosis stages. Alexa Fluor® 488 Annexin V/Dead Cell Apoptosis Kit was from Molecular Probes® (Eugene, OR, USA). Cells were exposed to doxepin at several concentrations for 24 h. Cells were harvested after incubation and washed in cold phosphate-buffered saline (PBS). Cells were resuspended in 400 μl reaction solution with 10 mM of HEPES, 140 mM of NaC1, 2.5 mM of $CaC1_2$ (pH 7.4). Alexa Fluor® 488 annexin V/PI staining solution was added in the dark. After incubation for 15 min, the cells were collected and analyzed in a FACScan flow cytometry analyzer. Excitation wavelength was at 488 nm and the emitted green fluorescence of Annexin V (FL1) and red fluorescence of PI (FL2) were collected using 530 nm and 575 nm band pass filters, respectively. A total of at least 20,000 cells were analyzed per sample. Light scatter was measured on a linear scale of 1024 channels and fluorescence intensity was on a logarithmic scale. The amount of early apoptosis and late apoptosis/necrosis were determined, respectively, as the percentage of Annexin V^+/PI^- or Annexin V^+/PI^+ cells.

Statistics

Data are reported as mean ± SEM of three separate experiments. Data were analyzed by one way analysis of variances (ANOVA) using the Statistical Analysis System (SAS®, SAS Institute Inc., Cary, NC, USA). Multiple comparisons between group means were performed by *post-hoc* analysis using the Tukey's HSD (honestly significantly difference) procedure. A *P*-value less than 0.05 was considered significant.

Results

Effect of Acute Treatment with Doxepin on $[Ca^{2+}]_i$ in PC3 Cells but not in MG63 Cells and DBTRG-05MG Cells

The effect of doxepin on basal $[Ca^{2+}]_i$ was examined. Fig. 1A shows that the basal $[Ca^{2+}]_i$ level was 51 ± 2 nM. At concentrations between 500 and 1000 μM, doxepin induced a $[Ca^{2+}]_i$ rise in a concentration-dependent manner in Ca^{2+}-containing medium. At a concentration of 1000 μM, doxepin evoked a $[Ca^{2+}]_i$ rise that attained to a net increase of 80 ± 2 nM (n = 3) followed by a slow decay. The Ca^{2+} response saturated at 1000 μM doxepin because 1250 μM doxepin did not evoke a greater response. Fig. 1B shows that in the absence of extracellular Ca^{2+}, 1000 μM doxepin induced a $[Ca^{2+}]_i$ rise of 55 ± 2 nM; and at a concentration of 750 μM, doxepin induced a $[Ca^{2+}]_i$ rise of 40 ± 2 nM. Fig. 1C shows the concentration-response plots of doxepin-induced responses. The EC_{50} value was 400 ± 2 μM or 760 ± 2 μM in the presence or absence of external Ca^{2+} by fitting to a Hill equation. Fig. 1D shows that doxepin between 100 μM and 1000 μM did not evoke a $[Ca^{2+}]_i$ rise in other cell types including MG63 cells and DBTRG-05MG cells.

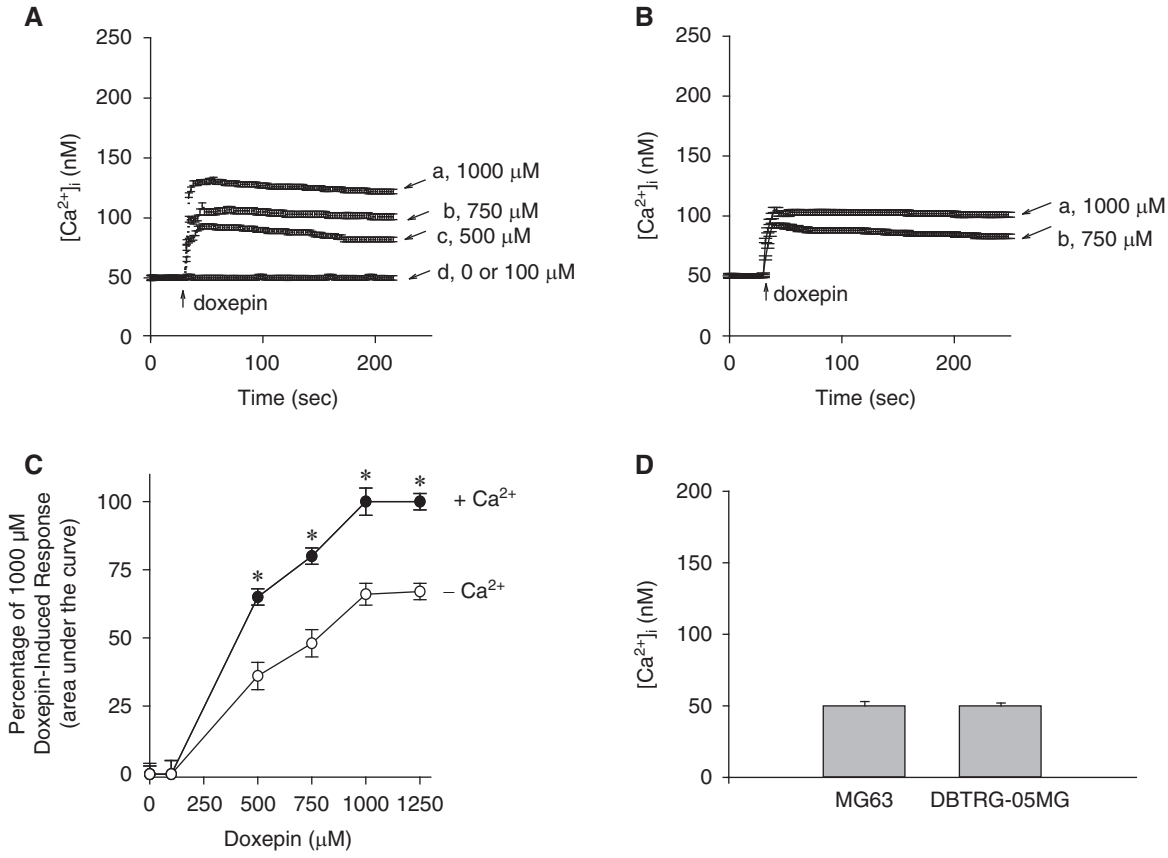

Fig. 1. Doxepin-induced $[Ca^{2+}]_i$ rises in PC3 cells. (A) Effect of doxepin on $[Ca^{2+}]_i$ in Ca^{2+}-containing medium. Doxepin was added at 25 sec. The concentration of doxepin was indicated. (B) Effect of doxepin on $[Ca^{2+}]_i$ in the absence of extracellular Ca^{2+}. Doxepin was added at 25 sec in Ca^{2+}-free medium. (C) Concentration-response plots of doxepin-induced $[Ca^{2+}]_i$ rises in the presence or absence of extracellular Ca^{2+}. Y axis is the percentage of the net (baseline subtracted) area under the curve (25-220 sec) of the $[Ca^{2+}]_i$ rise induced by 1000 μM doxepin in Ca^{2+}-containing medium. Data are mean ± SEM of three separate experiments. *$P < 0.05$ compared to open circles. (D) Doxepin (100-1000 μM) did not induce a $[Ca^{2+}]_i$ rise in MG63 human osteosarcoma cells and DBTRG-05MG human glioblastoma cells. Data are mean ± SEM of three separate experiments.

Effect of Ca^{2+} Channel Modulators on Doxepin-Induced $[Ca^{2+}]_i$ Rise

Fig. 1 shows that doxepin-induced Ca^{2+} response saturated at 1000 μM; thus in the following experiments the response induced by 1000 μM doxepin was used as control. Experiments were conducted to explore the Ca^{2+} entry pathway of the doxepin-induced $[Ca^{2+}]_i$ rise. The store-operated Ca^{2+} entry inhibitors: nifedipine (1 μM), econazole (0.5 μM) and SK&F96365 (5 μM); phorbol 12-myristate 13 acetate (PMA; 1 nM; a protein kinase C activator); and GF109203X (2 μM; a protein kinase C (PKC) inhibitor) were applied 1 min before doxepin. Addition of these chemicals (nifedipine, econazole, SK&F96365, PMA, GF109203X) alone did not alter baseline $[Ca^{2+}]_i$ (data not shown). These agents all significantly inhibited doxepin-induced $[Ca^{2+}]_i$ rise to different degree (Fig. 2).

Intracellular Store for Doxepin-Induced Ca^{2+} Release

Previous studies have shown that the endoplasmic reticulum is the major Ca^{2+} store in PC3 cells (4, 9). Fig. 3A shows that in Ca^{2+}-free medium, addition of 1000 μM doxepin induced a $[Ca^{2+}]_i$ rise of 50 ± 2 nM. Thapsigargin (1 μM), an inhibitor of endoplasmic reticulum Ca^{2+} pumps (32) was added afterwards. Thapsigargin failed to evoke a $[Ca^{2+}]_i$ rise (n = 3). Fig. 3B shows that addition of thapsigargin induced a $[Ca^{2+}]_i$ rise of 15 ± 2 nM (n = 3). Doxepin added afterwards induced a $[Ca^{2+}]_i$ rise of 45 ± 1 nM (n = 3) which was 10% smaller in the peak value ($P < 0.05$) than the control doxepin-induced response shown in Fig. 3A. To confirm the thapsigargin's data, another endoplasmic reticulum Ca^{2+} pump inhibitor 2,5-di-tert-butylhydroquinone (BHQ) (35) was used in similar experiments. Fig. 3C shows that BHQ added after doxepin induced a tiny transient $[Ca^{2+}]_i$ rise. Fig. 3D

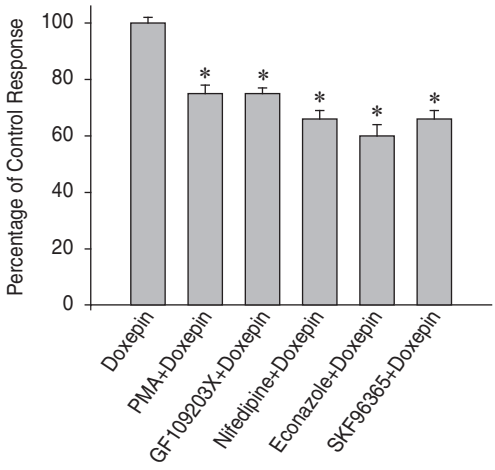

Fig. 2. Effect of Ca^{2+} channel modulators on doxepin-induced $[Ca^{2+}]_i$ rise. In blocker- or modulator-treated groups, the reagent was added 1 min before doxepin (1000 μM) in Ca^{2+}-containing medium. The concentration was 1 μM for nifedipine, 0.5 μM for econazole, 5 μM for SK&F96365, 10 nM for phorbol 12-myristate 13-acetate (PMA), and 2 μM for GF109203X. Data are expressed as the percentage of control (1st column) that is the maximum value of 1000 μM doxepin-induced $[Ca^{2+}]_i$ rise, and are mean ± SEM of three separate experiments. *$P < 0.05$ compared to the 1st column.

shows that BHQ induced a $[Ca^{2+}]_i$ rise of 45 ± 1 nM. Fig. 3D further shows that addition of doxepin after BHQ evoked a $[Ca^{2+}]_i$ rise of 40 ± 1 nM which was smaller than the control doxepin-induced response by 20%.

Lack of a Role of Phospholipase C (PLC) in Doxepin-Induced Ca^{2+} Release

PLC-dependent production of inositol 1,4,5-trisphosphate is a key process for releasing Ca^{2+} from the endoplasmic reticulum (1). Because doxepin released Ca^{2+} from the endoplasmic reticulum, the role of PLC in this event was examined. U73122, a PLC inhibitor (33), was used to see whether the activation of this enzyme was required for doxepin-induced Ca^{2+} release. It has been shown that ATP influenced biological processes *via* P2X purinoreceptors (3). P2X purinoreceptors are agonist-gated ion channels, while several P2Y receptors activate intracellular Ca^{2+} stores (2). Previous studies showed that ATP was used as a PLC-dependent agonist of $[Ca^{2+}]_i$ rise *via* P2X purinoreceptors in PC3 cells (3, 21). Therefore this study chose ATP to examine the role of PLC in PC3 cells. Fig. 4A shows that ATP (10 μM) induced a $[Ca^{2+}]_i$

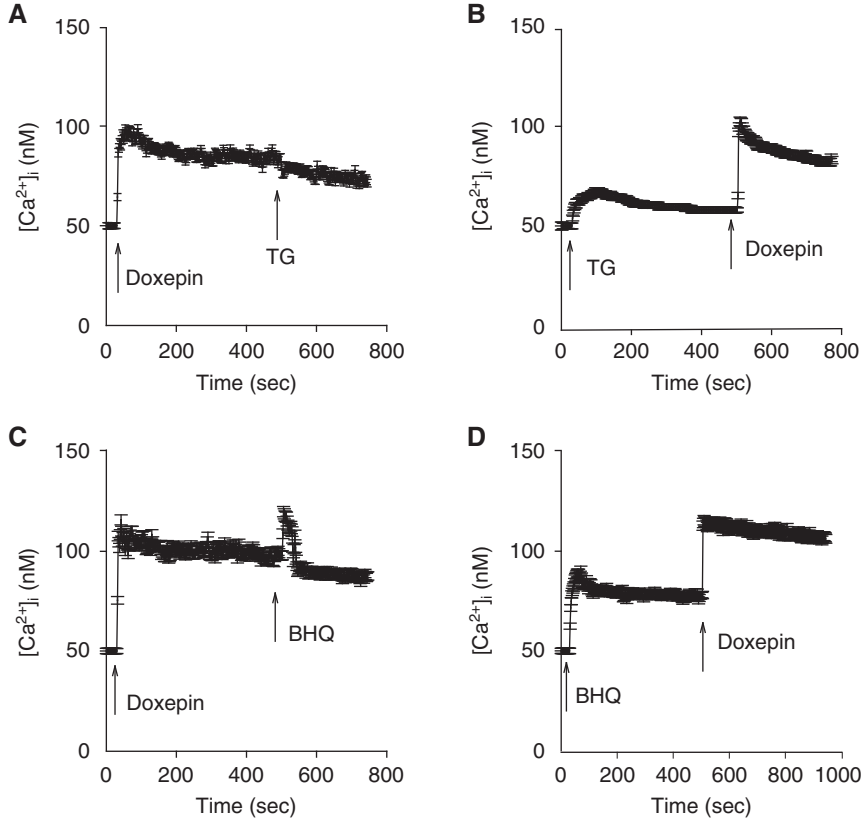

Fig. 3. Intracellular Ca^{2+} stores of doxepin-induced Ca^{2+} release. Experiments were performed in Ca^{2+}-free medium. Doxepin (1000 μM), thapsigargin (1 μM) and BHQ (50 μM) were added at time points indicated. Data are mean ± SEM of three separate experiments.

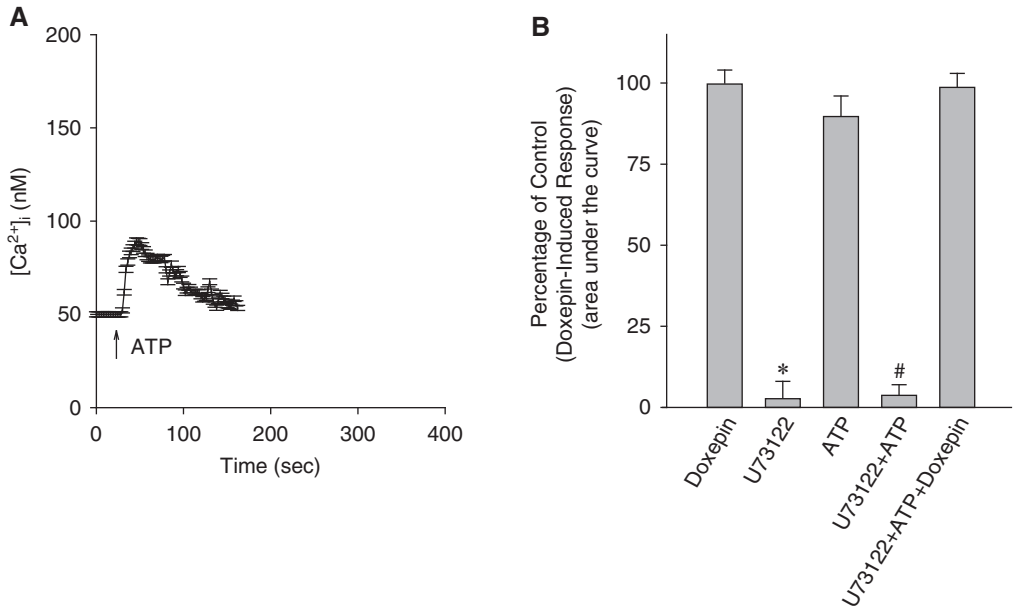

Fig. 4. Effect of U73122 on doxepin-induced Ca^{2+} release. Experiments were performed in Ca^{2+}-free medium. (A) ATP (10 μM) was added as indicated. (B) U73122 (2 μM), ATP (10 μM), and doxepin (1000 μM) were added as indicated. Data are mean ± SEM of three separate experiments.

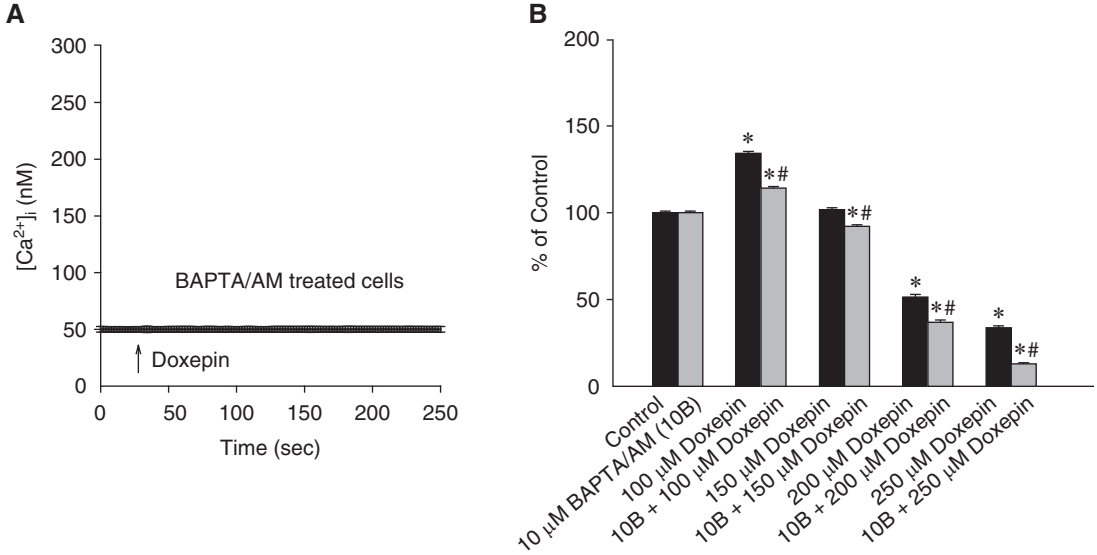

Fig. 5. Doxepin-induced Ca^{2+}-independent cell death. (A) Following BAPTA/AM treatment, cells were incubated with fura-2/AM as described in Methods. Then $[Ca^{2+}]_i$ measurements were conducted in Ca^{2+}-containing medium. Doxepin (500-1000 μM) was added as indicated. (B) Cells were treated with 0-250 μM doxepin for 24 h, and the cell viability assay was performed. Data are mean ± SEM of three separate experiments. Each treatment had six replicates (wells). Data are expressed as percentage of control that is the increase in cell numbers in doxepin-free groups. Control had 10,925 ± 712 cells/well before experiments, and had 13,951 ± 788 cells/well after incubation for 24 h. $^*P < 0.05$ compared to control. In each group, the Ca^{2+} chelator BAPTA/AM (10 μM) was added to cells followed by treatment with doxepin in Ca^{2+}-containing medium. Cell viability assay was subsequently performed. $^*P < 0.05$ compared to control. $^{\#}P < 0.05$ compared to the pairing group.

rise of 51 ± 2 nM. Fig. 4B shows that incubation with 2 μM U73122 did not change basal $[Ca^{2+}]_i$ but abolished ATP-induced $[Ca^{2+}]_i$ rise. This suggests that U73122 effectively suppressed PLC activity. Fig. 4B also shows that incubation with 2 μM U73122 did not alter basal $[Ca^{2+}]_i$ or doxepin-induced $[Ca^{2+}]_i$ rise. U73343 (2 μM), a U73122 analogue, failed to have an inhibition on ATP-induced $[Ca^{2+}]_i$ rise (not shown).

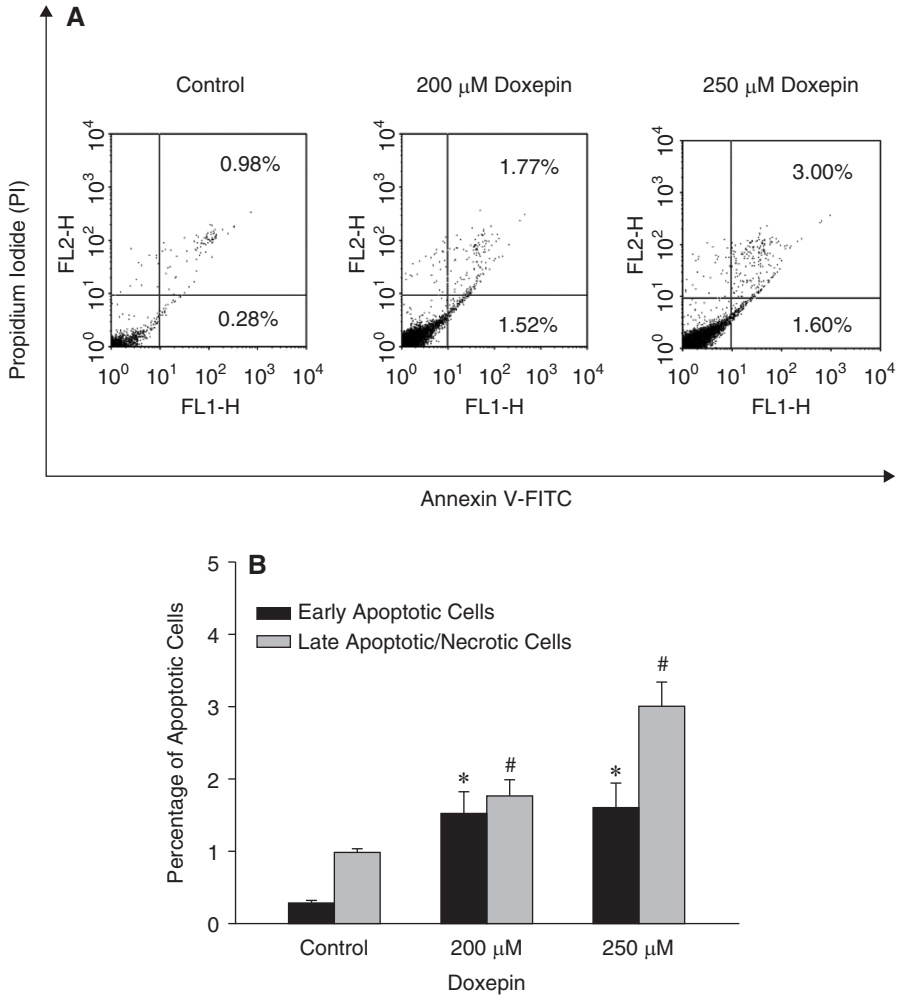

Fig. 6. Apoptosis induced by doxepin measured by Annexin V/PI staining. A. PC3 cells were treated with 0, 200 μM or 250 μM doxepin, respectively, for 24 h. Cells were then processed for Annexin V/PI staining and analyzed by flow cytometry. B. The percentage of apoptotic cells. $^{*,\#}P < 0.05$ compared to corresponding control.

Effect of Doxepin on Cell Viability

Given that acute incubation with doxepin induced a substantial and lasting $[Ca^{2+}]_i$ rise, and that unregulated $[Ca^{2+}]_i$ rise often alters cell viability (9), experiments were performed to examine the effect of doxepin on viability of PC3 cells. Cells were treated with 0-250 μM doxepin for 24 h, and the tetrazolium assay was performed. In the presence of 100 μM doxepin, cell viability increased by 30 ± 2%. In the presence of 200 or 250 μM doxepin, viability decreased in a concentration-dependent manner (Fig. 5).

Relationship between BAPTA/AM and Doxepin-Induced Changes in Viability

The next issue was whether the doxepin-induced changes in viability was caused by a preceding $[Ca^{2+}]_i$ rise. The intracellular Ca^{2+} chelator BAPTA/AM (34) was used to prevent a $[Ca^{2+}]_i$ rise during doxepin treatment. Previous studies showed that BAPTA/AM pretreatment at 10 μM abolished $[Ca^{2+}]_i$ rises in different cell types (10). In our study, Fig. 5A shows that 10 μM BAPTA/AM loading for 1 h abolished 1000 μM doxepin-induced $[Ca^{2+}]_i$ rise in Ca^{2+}-containing medium. Furthermore, 10 μM BAPTA/AM loading for 25 h also had the same results (data not shown). Therefore This suggests that BAPTA/AM effectively prevented a rise in $[Ca^{2+}]_i$ during doxepin treatment. Fig. 5B shows that 10 μM BAPTA/AM loading did not alter the control value of cell viability. BAPTA/AM loading did not reverse doxepin-induced changes in cell viability.

A Role of Apoptosis in Doxepin-Induced Cell Death

Because the cytotoxic response was most significant between 200 μM and 250 μM doxepin, these concentrations were chosen for apoptotic experiments. Annexin V/propidium iodide staining was applied to detect apoptotic cells after doxepin treatment. Figs. 6A

and 6B show that treatment with 200 μM or 250 μM doxepin did not induce significant apoptosis in PC3 cells.

Discussion

The effect of doxepin on Ca^{2+} signaling in cells has not been explored in any cell types. Our study shows that doxepin induced a $[Ca^{2+}]_i$ rise in PC3 human prostate cancer cells and examined the underlying mechanisms. This is the first report to show that doxepin increases $[Ca^{2+}]_i$ in a cultured cell model. The data show that doxepin induced a concentration-dependent $[Ca^{2+}]_i$ rise by depleting intracellular Ca^{2+} stores and causing Ca^{2+} entry from extracellular solution because removing extracellular Ca^{2+} partly decreased doxepin-induced $[Ca^{2+}]_i$ rise. In PC3 cells, about 66% of 1000 μM doxepin-evoked $[Ca^{2+}]_i$ rise was caused by Ca^{2+} release. In contrast, our data show that doxepin at a concentration of up to 1000 μM did not induce a $[Ca^{2+}]_i$ rise in MG63 cells and DBTRG-05MG cells. This suggests that doxepin-induced rise in $[Ca^{2+}]_i$ in PC3 cells is a noteworthy phenomenon.

The mechanism of doxepin-induced Ca^{2+} influx was explored. The results implicate that doxepin might induce Ca^{2+} influx *via* triggering store-operated Ca^{2+} entry, which is caused by depletion of intracellular Ca^{2+} stores (26), based on the inhibition of doxepin-induced $[Ca^{2+}]_i$ rise by nifedipine, econazole and SK&F96365. So far there are no selective blockers for this type of Ca^{2+} entry. These three compounds have often been applied to inhibit store-operated Ca^{2+} entry in different cell types (20, 22, 27, 29). Because activation of PLC produces IP_3 and diacylglycerol, which stimulates PKC, the effect of regulation of PKC activity on doxepin-induced $[Ca^{2+}]_i$ rise was examined. Both activation and inhibition of PKC inhibited doxepin-induced $[Ca^{2+}]_i$ rise. This suggests that a normal PKC activity is required for a full scale doxepin-induced $[Ca^{2+}]_i$ signal.

Regarding the Ca^{2+} stores involved in doxepin-induced Ca^{2+} release, the thapsigargin/BHQ-sensitive endoplasmic reticulum stores might be the dominant store because thapsigargin/BHQ pretreatment both greatly inhibited doxepin-induced $[Ca^{2+}]_i$ rise; and conversely, doxepin pretreatment also inhibited thapsigargin/BHQ-induced Ca^{2+} release. Since thapsigargin/BHQ treatment did not abolish doxepin-induced Ca^{2+} release, doxepin may release Ca^{2+} not only from endoplasmic reticulum, but also from other stores such as mitochondria, lysosomes, cytoskeleton, *etc*. However, it is difficult to explore this possibility because so far there are no chemicals to selectively release Ca^{2+} from these stores. It seems that PLC-dependent pathways did not play a significant role in doxepin-induced Ca^{2+} release, since the response was not inhibited when PLC activity was inhibited. Thus it appears that doxepin-induced Ca^{2+} release was caused by a PLC-independent Ca^{2+} release from the stores. The identity of this Ca^{2+} release is unclear. It is possible that doxepin could mimic thapsigargin/BHQ by inhibiting endoplasmic reticulum Ca^{2+} pump.

Doxepin has been shown to induce cell death in cultured dorsal root ganglion cells and malignant glioma (16, 18). This study shows that doxepin had a dual effect on viability of PC3 cells. At 100 μM, doxepin induced a 30% increase in viability. At higher concentrations of 200 and 250 μM doxepin, viability was decreased in a concentration-dependent manner.

It appears problematic that 1000 μM doxepin was required to induce a full blown $[Ca^{2+}]_i$ rise while 250 μM doxepin already caused death of 70% of cells. Note that $[Ca^{2+}]_i$ measurements and viability were two totally different assays. $[Ca^{2+}]_i$ measurements were conducted online and terminated within 4-15 min. After 20 min incubation with doxepin, cell viability was still >95%. In contrast, in viability assays, cells were treated with doxepin overnight in order to obtain measurable changes in viability. This is why 250 μM doxepin decreased cell viability in the tetrazolium assay by 70% whereas 1000 μM doxepin did not alter viability in $[Ca^{2+}]_i$ measurements.

Because doxepin induced both $[Ca^{2+}]_i$ rises and cell death, it would be interesting to know whether the death occurred in a Ca^{2+}-dependent manner. Chelation of cytosolic Ca^{2+} with BAPTA/AM did not reverse doxepin-induced changes in cell viability. Indeed, chelation of cytosolic Ca^{2+} even antagonized doxepin's action. This implies that in this case, doxepin's effect on cell viability was not downstream to a $[Ca^{2+}]_i$ rise. However, a Ca^{2+} signal can modulate cell viability in many cell types (9). It has been shown that Ca^{2+}-independent cell death could be found in some cell types such as macrophages (11) and human ovarian carcinoma cells (30). Although 250 μM doxepin caused cell death by 65% in viability experiments, the same concentration of doxepin did not induce significant apoptosis. Because Annexin V/PI staining showed a very low percentage of apopotic cells (3%), it appears that cell membrane was not disrupted. Doxepin induced cell death as indicated by the tetrazolium assay; however, this is not accompanied by the uptake of Annexin V/PI in the 24 h assay. Thus it is possible that the significant loss of cell viability was through other pathways such as autophagy.

Due to the rather high (hundreds of μM) concentrations of doxepin needed to induce a $[Ca^{2+}]_i$ rise and cell death, one logic concern is the clinical significance of our data. A previous study explored the plasma concentration of doxepin after oral administration. The doses administered were 25 and

75 mg/day in healthy adults. No BioResponse (BR) doxepin-related adverse effects were reported at doses up to 75 mg. A single 25 mg dose of BR-doxepin resulted in a mean C_{max} of ~ 200 μM after 4 h. A single 75 mg dose of BR-doxepin resulted in a mean C_{max} of ~ 400 μM after 4 h. BR-doxepin was well tolerated at single doses of up to 75 mg (13). However, in depression patients, the plasma concentration of doxepin after oral administration might be 2-fold higher than in healthy adults. Thus, our study may have clinical relevance.

Collectively, the results show that the antidepressant doxepin induced Ca^{2+} release from stores including endoplasmic reticulum in a PLC-independent manner and also caused Ca^{2+} influx *via* a PKC-dependent, store-operated Ca^{2+} entry in PC3 human prostate cancer cells. Doxepin also evoked cell proliferation or death depending on the concentration. This effect was independent of $[Ca^{2+}]_i$ rises. The possible effect on Ca^{2+} signaling and viability should be considered in performing other *in vitro* studies using doxepin.

Acknowledgments

This work was supported by grants from Kaohsiung Veterans General Hospital (VGHKS101-019) to Chung-Ren Jan, VGHKS13-CT5-08 and VGHKS100-115 to T Lu, and PS101001 to Wei-Chuan Chen.

The authors report no declarations of interest.

References

1. Bootman, M.D., Berridge, M.J. and Roderick, H.L. Calcium signalling: more messengers, more channels, more complexity. *Curr. Biol.* 12: R563-R565, 2002.
2. Burnstock, G. and Di Virgilio, F. Purinergic signalling and cancer. *Purinergic Signal*. 9: 491-540, 2013.
3. Calvert, R.C., Shabbir, M., Thompson, C.S., Mikhailidis, D.P., Morgan, R.J. and Burnstock, G. Immunocytochemical and pharmacological characterisation of P2-purinoceptor-mediated cell growth and death in PC-3 hormone refractory prostate cancer cells. *Anticancer Res*. 24: 2853-2860, 2004.
4. Chang, H.C., Cheng, H.H., Huang, C.J., Chen, W.C., Chen, I.S., Liu, S.I., Hsu, S.S., Chang, H.T., Wang, J.K., Lu, Y.C., Chou, C.T. and Jan, C.R. Safrole-induced Ca^{2+} mobilization and cytotoxicity in human PC3 prostate cancer cells. *J. Recept. Signal. Transduct. Res.* 26: 199-212, 2006.
5. Chang, H.C., Huang, C.C., Huang, C.J., Cheng, J.S., Liu, S.I., Tsai, J.Y., Chang, H.T., Huang, J.K., Chou, C.T. and Jan, C.R. Desipramine-induced apoptosis in human PC3 prostate cancer cells: activation of JNK kinase and caspase-3 pathways and a protective role of $[Ca^{2+}]_i$ elevation. *Toxicology* 250: 9-14, 2008.
6. Chang, K.H., Tan, H.P., Kuo, C.C., Kuo, D.H., Shieh, P., Chen, F.A. and Jan, C.R. Effect of nortriptyline on Ca^{2+} handling in SIRC rabbit corneal epithelial cells. *Chinese J. Physiol.* 53: 178-184, 2010.
7. Chen, W.C., Chou, C.T., Liou, W.C., Liu, S.I., Lin, K.L., Lu, T., Lu, Y.C., Hsu, S.S., Tsai, J.Y., Liao, W.C., Liang, W.Z. and Jan, C.R. Rise of $[Ca^{2+}]_i$ and apoptosis induced by *M*-3M3FBS in SCM1 human gastric cancer cells. *Chinese J. Physiol.* 57: 31-40, 2014.
8. Cheng, J.S., Lo, Y.K., Yeh, J.H., Cheng, H.H., Liu, C.P., Chen, W.C. and Jan, C.R. Effect of gossypol on intracellular Ca^{2+} regulation in human hepatoma cells. *Chinese J. Physiol.* 46: 117-122, 2003.
9. Clapham, D.E. Intracellular calcium. Replenishing the stores. *Nature* 375: 634-635, 1995.
10. Collatz, M.B., Rüdel, R. and Brinkmeier, H. Intracellular calcium chelator BAPTA protects cells against toxic calcium overload but also alters physiological calcium responses. *Cell Calcium* 21: 453-459, 1997.
11. Costa-Junior, H.M., Mendes, A.N., Davis, G.H., da Cruz, C.M., Ventura, A.L., Serezani, C.H., Faccioli, L.H., Nomizo, A., Freire-de-Lima, C.G., Bisaggio Rda, C. and Persechini, P.M. ATP-induced apoptosis involves a Ca^{2+}-independent phospholipase A_2 and 5-lipoxygenase in macrophages. *Prostaglandins Other Lipid Mediat.* 88: 51-61, 2009.
12. Duncan, R.S., McPate, M.J., Ridley, J.M., Gao, Z., James, A.F., Leishman, D.J., Leaney, J.L., Witchel, H.J. and Hancox, J.C. Inhibition of the HERG potassium channel by the tricyclic antidepressant doxepin. *Biochem. Pharmacol.* 74: 425-437, 2007.
13. Geister, U., Gaupp, M., Arnold, P., Schaarschmidt, D., Doser, K. and Renner, J. Bioavailability investigation of two different oral formulations of doxepin. *Arzneimittel-Forschung* 51: 189-196, 2001.
14. Gillman, P.K. Tricyclic antidepressant pharmacology and therapeutic drug interactions updated. *Brit. J. Pharmacol.* 151: 737-748, 2007.
15. Grynkiewicz, G., Poenie, M. and Tsien, R.Y. A new generation of Ca^{2+} indicators with greatly improved fluorescence properties. *J. Biol. Chem.* 260: 3440-3450, 1985.
16. Haller, I., Lirk, P., Keller, C., Wang, G.K., Gerner, P. and Klimaschewski, L. Differential neurotoxicity of tricyclic antidepressants and novel derivatives *in vitro* in a dorsal root ganglion cell culture model. *Eur. J. Anaesthesiol.* 24: 702-708, 2007.
17. Hertz, L., Richardson, J.S. and Mukerji, S. Doxepin, a tricyclic antidepressant, binds to normal, intact astroglial cells in cultures and inhibits the isoproterenol-induced increase in cyclic AMP production. *Can. J. Physiol. Pharmacol.* 58: 1515-1519, 1980.
18. Higgins, S.C. and Pilkington, G.J. The *in vitro* effects of tricyclic drugs and dexamethasone on cellular respiration of malignant glioma. *Anticancer Res.* 30: 391-397, 2010.
19. Huang, J.K., Huang, C.C., Lu, T., Chang, H.T., Lin, K.L., Tsai, J.Y., Liao, W.C., Chien, J.M. and Jan, C.R. Effect of MK-886 on Ca^{2+} level and viability in PC3 human prostate cancer cells. *Basic Clin. Pharmacol. Toxicol.* 104: 441-447, 2009.
20. Ishikawa, J., Ohga, K., Yoshino, T., Takezawa, R., Ichikawa, A., Kubota, H. and Yamada, T. A pyrazole derivative, YM-58483, potently inhibits store-operated sustained Ca^{2+} influx and IL-2 production in T lymphocytes. *J. Immunol.* 170: 4441-4449, 2009.
21. Janssens, R. and Boeynaems, J.M. Effects of extracellular nucleotides and nucleosides on prostate carcinoma cells. *Brit. J. Pharmacol.* 132: 536-546, 2001.
22. Jiang, N., Zhang, Z.M., Liu, L., Zhang, C., Zhang, Y.L. and Zhang, Z.C. Effects of Ca^{2+} channel blockers on store-operated Ca^{2+} channel currents of Kupffer cells after hepatic ischemia/reperfusion injury in rats. *World J. Gastroenterol.* 12: 4694-4698, 2006.
23. Kitamura, Y., Arima, T., Kitayama, Y. and Nomura, Y. Regulation of $[Ca^{2+}]_i$ rise activated by doxepin-sensitive H_1-histamine receptors in Jurkat cells, cloned human T lymphocytes. *Gen. Pharmacol.* 27: 285-291, 1996.
24. Nakashita, M., Sasaki, K., Sakai, N. and Saito, N. Effects of tricyclic and tetracyclic antidepressants on the three subtypes of GABA transporter. *Neurosci. Res.* 29: 87-91, 1997.
25. Pancrazio, J.J., Kamatchi, G.L., Roscoe, A.K. and Lynch, C. 3rd: Inhibition of neuronal Na^+ channels by antidepressant drugs. *J. Pharmacol. Exp. Ther.* 284: 208-214, 1998.
26. Putney, J.W. Jr. A model for receptor-regulated calcium entry. *Cell Calcium* 7: 1-12, 1986.

27. Quinn, T., Molloy, M., Smyth, A. and Baird, A.W. Capacitative calcium entry in guinea pig gallbladder smooth muscle *in vitro*. *Life Sci.* 74: 1659-1669, 2004.
28. Roth, J.A. Inhibition of rabbit monoamine oxidase by doxepin and related drugs. *Life Sci.* 16: 1309-1319, 1975.
29. Shideman, C.R., Reinardy, J.L. and Thayer, S.A. γ-Secretase activity modulates store-operated Ca^{2+} entry into rat sensory neurons. *Neurosci. Lett.* 451: 124-128, 2009.
30. Song, Y., Wilkins, P., Hu, W., Murthy, K.S., Chen, J., Lee, Z., Oyesanya, R., Wu, J., Barbour, S.E. and Fang, X. Inhibition of calcium-independent phospholipase A_2 suppresses proliferation and tumorigenicity of ovarian carcinoma cells. *Biochem. J.* 406: 427-436, 2007.
31. Thase, M.E. New directions in the treatment of atypical depression. *J. Clin. Psychiatry* 67: e18, 2006.
32. Thastrup, O., Cullen, P.J., Drøbak, B.K., Hanley, M.R. and Dawson, A.P. Thapsigargin, a tumor promoter, discharges intracellular Ca^{2+} stores by specific inhibition of the endoplasmic reticulum Ca^{2+}-ATPase. *Proc. Natl. Acad. Sci. USA* 87: 2466-2470, 1990.
33. Thompson, A.K., Mostafapour, S.P., Denlinger, L.C., Bleasdale, J.E. and Fisher, S.K. The aminosteroid U-73122 inhibits muscarinic receptor sequestration and phosphoinositide hydrolysis in SK-N-SH neuroblastoma cells: a role for Gp in receptor compartmentation. *J. Biol. Chem.* 266: 23856-23862, 1991.
34. Tsien, R.Y. New calcium indicators and buffers with high selectivity against magnesium and protons: design, synthesis, and properties of prototype structures. *Biochemistry* 19: 2396-2404, 1980.
35. Wassenberg, J.J., Clark, K.D. and Nelson, D.L. Effect of SERCA pump inhibitors on chemoresponses in *Paramecium*. *J. Eukaryotic Microbiol.* 44: 574-581, 1997.
36. Weber, J., Siddiqui, M.A., Wagstaff, A.J. and McCormack, P.L. Low-dose doxepin: in the treatment of insomnia. *CNS Drugs* 24: 713-720, 2010.
37. Wen, Z., Pyeon, D., Wang, Y., Lambert, P., Xu, W. and Ahlquist, P. Orphan nuclear receptor PNR/NR2E3 stimulates p53 functions by enhancing p53 acetylation. *Mol. Cell. Biol*. 32: 26-35, 2012.